subsurface weathering zone. The longevity of these less coherent surface boulders is reduced, which together with the selective disappearance of older boulders decreases the mean exposure age of surface boulders. The possibility that mean exposure ages of boulders on the crest of a younger moraine could exceed those on an older moraine was apparently not considered by Phillips and co-workers (*5*), who interpreted their cosmogenic dates as suggesting that the previously accepted chronology for the older moraines should be reversed (Fig. 2A).

Factors absent from the model, such as the attritional loss of cosmogenically enriched outer parts of boulders and prior exposure, introduce additional uncertainty into the interpretation of cosmogenic surface exposure ages. In view of these complications and uncertainties, chronologies based on cosmogenically determined boulder ages may generally differ from lateral moraine-age sequences that are based on geomorphic arguments and stratigraphy. Such differences, rather than complete accord, are to be expected, particularly for older moraines. Contrary to common assertions (*14*), moraines with identical exposure ages are not necessarily correlative (Fig. 2B).

Our model yields considerable insight into the diverse consequences of erosion and weathering on exposure-age dating of moraines and provides ample motivation for refining the modeling of these processes. More generally, our theoretical considerations highlight the need to complement advances in the use of cosmogenic isotopes to date geomorphic surfaces with detailed examination of the dynamic nature of landforms and of the universally present processes of weathering, erosion, and deposition.

REFERENCES AND NOTES

1. D. Lal, *Annu. Rev. Earth Planet. Sci.* **16**, 355 (1988).
2. P. R. Bierman, *J. Geophys. Res.*, in press.
3. K. Nishiizumi *et al.*, *ibid.* **94**, 907 (1989).
4. A. R. Gillespie and P. R. Bierman, unpublished results.
5. F. M. Phillips *et al.*, *Science* **248**, 1529 (1990).
6. E. Blackwelder, *Geol. Soc. Am. Bull.* **42**, 865 (1931).
7. R. P. Sharp and J. H. Birman, *ibid.* **74**, 1079 (1963).
8. R. M. Burke and P. W. Birkeland, *Quat. Res.* **11**, 21 (1979).
9. A. R. Gillespie, thesis, California Institute of Technology (1982); R. Crook and A. R. Gillespie, in *Rates of Chemical Weathering of Rocks and Minerals*, S. M. Colman and D. P. Dethier, Eds. (Academic Press, San Diego, CA, 1986), pp. 395–417.
10. M. I. Bursik and A. R. Gillespie, *Quat. Res.* **39**, 24 (1993).
11. P. W. Birkeland and R. M. Burke, *Arct. Alp. Res.* **20**, 473 (1988).
12. The local mean annual precipitation is 450 mm. Modern vegetation consists of mixed conifer forest with an understory of Great Basin sage community.
13. P. Bierman and A. Gillespie, *Geology* **19**, 641 (1991).
14. M. G. Zreda and F. M. Phillips, *Eos* (fall meeting) **74**, 292 (abstr.) (1993).
15. S. M. Colman and K. L. Pierce, *Quat. Res.* **25**, 25 (1986).
16. T. C. Meierding, in *Correlation of Quaternary Chronologies*, W. C. Mahaney, Ed. (Geo Books, Norwich, UK, 1984), pp. 455–477.
17. R. S. Anderson and N. F. Humphrey, in *Quantitative Dynamic Stratigraphy*, T. A. Cross, Ed. (Prentice-Hall, Englewood Cliffs, NJ, 1989), chap. 19. For a more general introduction to diffusional modeling of topography, see M. A. Carson and M. J. Kirkby, *Hillslope Form and Process* (Cambridge Univ. Press, New York, 1972).
18. Boulders are assumed not to move downslope because erosional processes that probably dominate in transferring material downslope in this climatic region (soil creep, wind scour, rain splash) operate on a scale much smaller than that needed to move boulders. Field observations support this assumption: If boulders were moving downslope they would accumulate at the foot of the moraine, but this is not the case.
19. This relation is applicable for any soil-moving process and for motion restricted down the fall line, which is appropriate because lateral moraines are long ridges adequately modeled by the consideration of only the soil transfer perpendicular to the moraine axis.
20. K. L. Pierce and S. M. Colman, *Geol. Soc. Am. Bull.* **97**, 869 (1986). The κ increase with slope length presumably reflects the increasing importance of slope length–dependent sediment transport by sheet wash and rilling.
21. T. C. Hanks *et al.*, *J. Geophys. Res.* **89**, 5771 (1984).
22. T. Swanson, personal communication.
23. R. P. Sharp, *Geol. Soc. Am. Bull.* **83**, 2233 (1972).
24. We thank A. Gillespie for his interest and encouragement; T. Swanson for his unpublished topographic profiles; and D. Clark, A. Heyneman, T. Swanson, and especially A. Gillespie for thoughtful reviews and suggestions. Supported by the National Science Foundation and Academy of Finland.

22 March 1994; accepted 29 June 1994

Controlling Molecular Order in "Hairy-Rod" Langmuir-Blodgett Films: A Polarization-Modulation Microscopy Study

V. K. Gupta, J. A. Kornfield,* A. Ferencz, G. Wegner

The interplay of molecular weight, layer thickness, and thermal annealing in controlling molecular order in ultrathin Langmuir-Blodgett films is characterized with the use of polarization-modulation laser-scanning microscopy. The degree and direction of molecular alignment can be imaged rapidly and sensitively through the magnitude and orientation of linear dichroism in Langmuir-Blodgett films of rodlike poly(phthalocyaninatosiloxane) (PcPS). Images are presented for films as thin as two molecular layers (~44 angstroms). Molecular alignment along the transfer direction is much stronger for films of PcPS with ~25 repeat units (~10 nanometers long) than for those with ~50 repeat units (~20 nanometers long). Enhancement of alignment by thermal annealing is also much greater for PcPS-25 than PcPS-50. Intimate interaction with the substrate suppresses improvement in alignment by annealing, evident by an anomalously small increase in anisotropic absorption of the first two layers.

Molecular orientation plays a key role in the combined areas of polymer physics, condensed matter physics, and thin-film technology because it determines the useful properties of a large class of materials. For example, a high degree of alignment is the basis of improved mechanical, optical, and electrical properties in almost all polymers and in the technological application of liquid crystalline and other mesoscale-ordered systems. Consequently, it is necessary to understand the correlations among molecular order, material properties, and fabrication procedures. Toward this end, we developed an optical technique to image molecular order and study Langmuir-Blodgett (LB) films of a rigid-rod polymer.

The high degree of order in LB films opens potential applications as nonlinear optical systems, molecular templates for protein crystallization, insulating or patterning layers in microelectronic devices, and selective layers in biosensors (*1*). Experimental characterization of the degree and direction of alignment in films as thin as a few nanometers is required in order to understand how molecular design and processing strategies lead to the ultimate state of alignment.

Various spectroscopic methods have been used to examine the structure, properties, and molecular arrangement of LB films (*1*, *2*); however, detailed characterization of molecular order has been lacking because these spectroscopic techniques average over large areas of films a

---

V. K. Gupta and J. A. Kornfield, Division of Chemistry and Chemical Engineering, California Institute of Technology, Pasadena, CA 91125, USA.
A. Ferencz and G. Wegner, Max-Planck-Institut für Polymerforschung, Postfach 3148, D-6500 Mainz, Germany.

*To whom correspondence should be addressed.

few layers thick. Information at molecular resolution can be obtained by direct imaging with transmission or scanning electron microscopy (TEM or SEM) (*3–6*), scanning tunneling microscopy (STM) (*3, 7, 8*), or atomic force microscopy (AFM) (*7, 9*), but only for a limited number of systems. Compounds that typically form LB films cannot withstand the irradiation in TEM or SEM, and even for organic compounds that are hardy enough, low dose imaging is required. Films have to be prepared on special electron microscope (metal) grids covered with carbon, which involves significant changes in either the deposition procedures (film flotation or horizontal deposition) or in the deposition dynamics (dipping of grid-attached substrates). As most LB films are insulating, investigation with STM has to be performed on conductive substrates. Imaging with AFM requires that molecules of interest be rigidly mounted and immobilized with well-defined orientation to avoid damage by physical contact. Because the complex microstructure in these organic films depends intricately on a combination of molecular structure, deposition dynamics, substrate properties, and post-treatment, meaningful structure-property relations have to be established under conditions closer to those in potential manufacturing processes. Therefore, techniques such as TEM, SEM, STM, and AFM are unsuitable for the characterization of molecular alignment that is required to study these relations. In contrast, optical measurement techniques are noninvasive and nondestructive, have fast response times and high sensitivity, and can be used to perform measurements under ambient conditions. However, established optical tools cannot perform quantitative imaging of molecular order in ultrathin films.

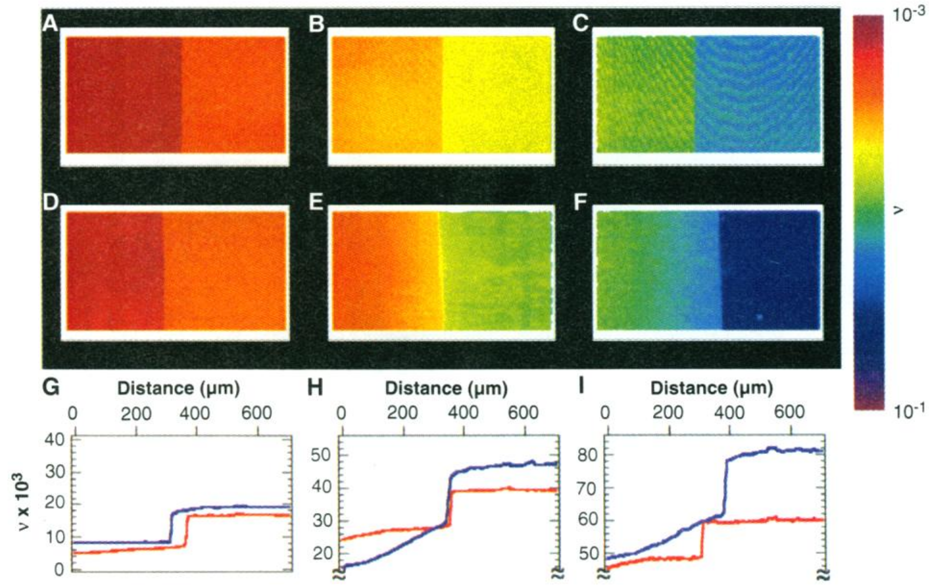

Fig. 1. Linear dichroism field at the boundaries between two regions covered with different numbers of molecular layers of PcPS-25. The anisotropy in absorption (ν) has been color-coded from dark red to dark blue as the magnitude increases (see color scale). (**A** through **C**) Images of the unannealed sample. (**D** through **F**) Images after annealing. (**G** through **I**) Vertical line averages of ν as a function of distance along the image (red, unannealed sample; blue, annealed). In (A), (D), and (G), the boundary is between bare glass and two layers. In (B), (E), and (H), the boundary is at the two- to four- layer edge. In (C), (F), and (I), the boundary is at the four- to six-layer edge.

We have addressed the need for rapid, sensitive imaging of molecular orientation by developing polarization-modulation laser-scanning microscopy (PM-LSM). This method allows us to image the optical anisotropy (dichroism, the anisotropic absorption, and birefringence, the anisotropic retardation) of materials with polarized light. In structurally anisotropic materials, the magnitude and orientation of the optical anisotropy can be directly related to the orientational correlation that exists in the material, in particular, the orientation of the optical axis and the degree of order. Thus, it becomes possible to quantify the orientation field in the sample by the pattern of birefringence or dichroism that is observed. We have combined scanning optical microscopy (*10*) and polarization-modulation polarimetry (*11*) to perform simultaneous acquisition of both the magnitude and orientation of the birefringence or dichroism (*12*). Because it uses a bright, monochromatic, collimated source, the laser scanning system intrinsically provides significantly greater sensitivity and higher speed of image acquisition (more than 2000 pixels per second) than previous techniques. We have used PM-LSM to image, pixel by pixel, the molecular order in LB films as thin as two molecular layers (~44 Å).

We investigated the interplay of molecular properties and surface interactions in the determination of molecular order in deposited films and its manipulation by subsequent processing steps. To achieve this end, we imaged the molecular orientation and order in ultrathin LB films of a "hairy-rod" polymer that has asymmetrically alkoxy-substituted phthalocyanines linked together by a siloxane backbone [tetra(methoxy)-tetra(octyloxy)-phthalocyaninatopolysiloxane (PcPS)] (*13, 14*). The phthalocyanine-based rodlike polymers are ideal candidates because the phthalocyanine molecule is a dye that is optically anisotropic. Under visible light, PcPS absorbs strongly and exhibits a maximum absorption anisotropy at wavelengths around 550 nm. Cofacial arrangement of the phthalocyanine rings with siloxane linkages results in anisotropy with a principal axis along the rod. Wegner and co-workers have found that in deposited films of asymmetrically substituted phthalocyaninato-polysiloxane, the rodlike molecule lies in an orientationally ordered state (*5, 13, 15*).

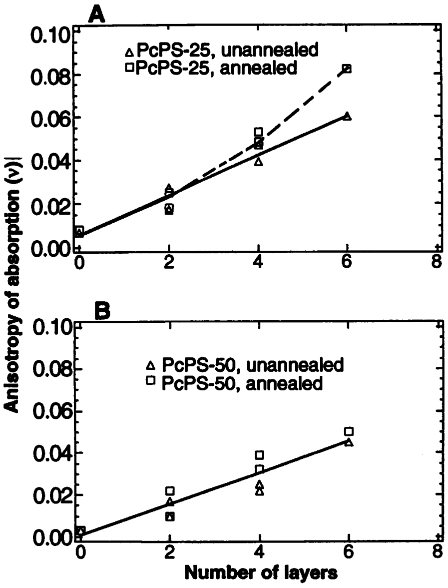

Fig. 2. Anisotropy of absorption (ν) for different layer thickness in as-deposited and annealed LB films of (**A**) PcPS-25 and (**B**) PcPS-50. The solid and dashed curves are drawn to guide the eye.

To study the effect of molecular weight, we prepared films of PcPS with ~25 (PcPS-25) and ~50 (PcPS-50) repeat units (estimated from high-resolution electron micrographs). To understand the variation of molecular order

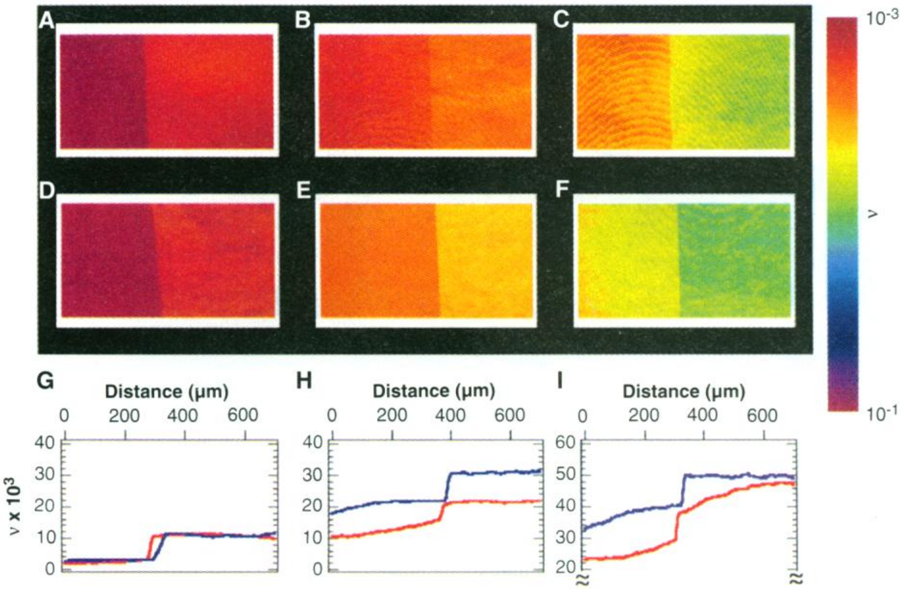

Fig. 3. Linear dichroism field at the boundaries between two regions covered with different numbers of molecular layers for the PcPS-50. The anisotropy in absorption has been color-coded with the same scale as in Fig. 1. (**A** through **C**) Images of the unannealed sample. (**D** through **F**) Images after annealing. (**G** through **I**) Vertical line averages of ν as a function of distance along the image (red, unannealed sample; blue, annealed). In (A), (D), and (G), the boundary is between bare glass and two layers. In (B), (E), and (H), the boundary is at the two- to four-layer edge. In (C), (F), and (I), the boundary is at the four- to six-layer edge.

with the interaction between layers and between layers and the substrate, we studied samples of both molecular weights in films of two, four, and six molecular layers. To characterize the enhancement of molecular alignment on thermal annealing and its relation to molecular weight and layer stacking, we compared unannealed samples with samples annealed at 120°C for 1 hour for both sets of polymers and each series of molecular layers.

The PcPS molecules were spread on a Lauda film balance at 6°C, and the monolayer was compressed to a deposition surface pressure of 25 mN/m. We deposited two, four, and six layers onto microscope glass slides by dipping the slide to different lengths at a speed of 10 mm/min. Each dipping cycle included a 20-min upper stop relaxation (drying) time with nitrogen flowing. Using PM-LSM at 543 nm, we imaged the anisotropy of absorption $\nu = (A_{\parallel} - A_{\perp})/2$, where $A_{\parallel}$ is the absorption parallel to the transfer direction and $A_{\perp}$ is the absorption perpendicular to the transfer direction, and where ν is proportional to the magnitude of linear dichroism. Images of ν characterize the degree of molecular order and thickness, whereas its orientation angle coincides with the mean direction of alignment of the backbone of PcPS.

The LB films have extremely homogeneous orientational order, indicated by the uniformity of ν in deposited layers of PcPS-25 (Fig. 1, A through F). This homogeneous order improves in general upon thermal annealing (Fig. 1, A through C versus D through F). However, this increase in ν for the molecular layers is modified by the interaction with the underlying surface. This effect is manifested as an almost imperceptible increase in ν for the region covered with two molecular layers (Fig. 1, A and D). In contrast, the degree of molecular reorientation is larger in successive layers of the LB film (Fig. 1, B versus E and C versus F). This change can be seen easily in the line averages in Fig. 1G, where the step jump in going from bare glass to a region of two layers remains almost unchanged after annealing, and is in distinct contrast to change in the step heights in Fig. 1, H and I. Intimate interaction between the substrate surface and adjacent layers strongly affects the refinement of order, and the strength of this interaction decays with layer thickness (Fig. 2A). Beyond as few as four layers, the degree of reorientation during annealing becomes insensitive to the presence of the substrate.

The longer PcPS-50 also exhibits increasing ν with an increase from two to six molecular layers. However, in comparison to the shorter PcPS-25, the anisotropy of absorption for each film thickness is significantly lower in PcPS-50 films. The region covered with two molecular layers shows almost no increase in ν upon annealing (Fig. 3, A, D, and G), and only a slight increase becomes apparent in layers that are built up on a foundation of a few multilayers of PcPS (Fig. 3, B and C, E and F, and H and I). Because longer rodlike molecules generally have a higher degree of local order, this decrease in alignment with increasing molecular weight suggests a reduction in the mesoscale order in transferred films from PcPS-25 to PcPS-50. The order in the transferred film of PcPS-50 is not only lower than that of PcPS-25 but also is less amenable to refinement with annealing (Fig. 2B). Again, this difference may suggest that mesoscale disorder is present. Thermal treatment may increase alignment within domains in the PcPS-50 films; however, if these domains have a wide distribution of orientation, no macroscopic improvement in alignment is achieved by annealing.

REFERENCES AND NOTES

1. J. D. Swalen *et al.*, *Langmuir* **3**, 932 (1987); G. G. Roberts, *Langmuir-Blodgett Films* (Plenum, New York, 1990).
2. P. Chollet, *Thin Solid Films* **68**, 13 (1980); P. Chollet and J. Messier, *ibid.* **99**, 197 (1983).
3. H. G. Braun, H. Fuchs, W. Schrepp, *ibid.* **159**, 301 (1988).
4. J. R. Fryer, R. A. Hann, B. L. Eyres, *Nature* **313**, 382 (1985); N. Uyeda, T. Takenaka, K. Aoyama, M. Matsumoto, Y. Fujiyoshi, *ibid.* **327**, 319 (1987); R. D. Neuman and S. Fereshtehkhou, *J. Colloid Interface Sci.* **125**, 34 (1988).
5. K. Yase, S. Schwiegk, G. Lieser, G. Wegner, *Thin Solid Films* **210–211**, 22 (1992).
6. F. W. Embs, E. L. Thomas, A. Gittinger, L. Dulog, *ibid.* **237**, 217 (1994).
7. T. R. Albrecht *et al.*, *J. Appl. Phys.* **64**, 1178 (1988).
8. J. P. Rabe, M. Sano, D. Batchelder, A. A. Kalatchev, *J. Microsc.* **152**, 573 (1988); J. H. Coombs, J. B. Pethica, M. E. Welland, *Thin Solid Films* **159**, 293 (1988).
9. E. Meyer *et al.*, *Nature* **349**, 398 (1991); J. A. N. Zasadzinski, C. A. Helm, M. L. Longo, S. A. C. Gould, P. K. Hansma, *Biophys. J.* **59**, 755 (1991); L. F. Chi, M. Anders, H. Fuchs, R. R. Johnston, H. Ringsdorf, *Science* **259**, 213 (1993); J. Y. Josefowicz *et al.*, *ibid.* **260**, 323 (1993); J. A. Zasadzinski, R. Viswanathan, L. Madsen, J. Garnaes, D. K. Schwartz, *ibid.* **263**, 1726 (1994).
10. C. J. Sheppard and T. Wilson, *Theory and Practice of Optical Scanning Microscopy* (Academic Press, New York, 1985); V. Wilke, *Proc. SPIE* **396**, 164 (1984); V. Wilke, *Scanning* **7**, 88 (1985).
11. R. A. Azzam and N. M. Bashara, *Ellipsometry and Polarized Light* (North-Holland, Amsterdam, 1987); J. A. Schellman, *Polarized Spectroscopy of Ordered Systems*, B. Samori and W. Thulstrup, Eds. (Kluwer Academic, Dordrecht, Netherlands, 1987); G. G. Fuller, *Annu. Rev. Fluid Mech.* **22**, 387 (1990); S. J. Johnson, P. L. Frattini, G. G. Fuller, *J. Colloid Interface Sci.* **104**, 440 (1985).
12. V. K. Gupta and J. A. Kornfield, *Rev. Sci. Instrum.*, in press.
13. E. Orthmann and G. Wegner, *Angew. Chem. Int. Ed. Engl.* **25**, 1105 (1986).
14. G. Duda *et al.*, *Thin Solid Films* **159**, 221 (1988); G. Duda and G. Wegner, *Makromol. Chem. Rapid Commun.* **9**, 495 (1988).
15. T. Sauer, T. Arndt, D. N. Batchelder, A. A. Kalachev, G. Wegner, *Thin Solid Films* **187**, 357 (1990).
16. The ridges in Figs. 1C and 3, B and C, are an optical artifact and are not intrinsic to the sample.
17. Supported by Raychem and the Caltech Consortium in Chemistry and Chemical Engineering: E. I. duPont de Nemours, Eastman Kodak, and 3M.

27 April 1994; accepted 27 June 1994